Modeling of Hysteresis Losses in Ferromagnetic Laminations under Mechanical Stress

P. Rasilo[1], D. Singh[1], U. Aydin[1], F. Martin[1], R. Kouhia[2], A. Belahcen[1], A. Arkkio[1]

[1]Department of Electrical Engineering and Automation, Aalto University, Espoo, Finland
[2]Department of Mechanical Engineering and Industrial Systems, Tampere University of Technology, Tampere, Finland
paavo.rasilo@aalto.fi

A novel approach for predicting magnetic hysteresis loops and losses in ferromagnetic laminations under mechanical stress is presented. The model is based on combining an energy-based anhysteretic magnetoelastic constitutive law to a vector Jiles-Atherton hysteresis model. The hysteresis loops and losses are modeled accurately for stresses ranging from -50 to 80 MPa.

***Index Terms*—Helmholtz free energy, magnetic hysteresis, magnetoelasticity, magnetostriction, strain, stress.**

I. Introduction

DEPENDENCY of iron losses on mechanical stresses and strains remains a problem in accurate design and analysis of electrical machines. The increase of power losses due to mechanical processing of the core laminations [1] is generally associated to the deformations and residual stresses caused by the process. In addition, temperature gradients and centrifugal forces give rise to additional mechanical loadings in the cores.

Different approaches for both theoretical [2]-[3] and experimental [4]-[5] formulations for coupled multiaxial magnetomechanical field problems have been presented quite recently. However, modeling of the losses has received less attention, and the presented loss models have typically been based on large amounts of experimental data. For example in [1] and [5], measured iron-loss and magnetization curves were used in finite-element (FE) analysis to study the effects of shrink-fitting and punching in electrical machine stator cores.

In [6], an interesting approach was taken to couple the single-valued constitutive law of [3] to the vector Jiles-Atherton (J-A) hysteresis model. In this paper, we implement a somewhat similar extension for the model of [2]. The model gives promising results when initially fitted to measurements under unidirectional flux density and stress.

II. Methods

The flux density vector $\boldsymbol{B}$ and the total strain tensor $\boldsymbol{\varepsilon}$ are chosen as the independent variables, as functions of which the magnetization $\boldsymbol{M}$ and the total stress $\boldsymbol{\sigma}$ are to be derived. Following [2], a Helmholtz free energy density $\psi(I_1, I_2, I_4, I_5, I_6)$ is first expressed analytically as a function of the following five invariants:

$$I_1 = \operatorname{tr}\boldsymbol{\varepsilon},\ I_2 = \frac{1}{2}\operatorname{tr}\boldsymbol{\varepsilon}^2$$
$$I_4 = \boldsymbol{B}\cdot\boldsymbol{B},\ I_5 = \boldsymbol{B}\cdot\left(\boldsymbol{\varepsilon}\boldsymbol{B}\right),\ I_6 = \boldsymbol{B}\cdot\left(\boldsymbol{\varepsilon}^2\boldsymbol{B}\right). \tag{1}$$

The single-valued (SV) magnetization and the magnetostrictive stress are then calculated as partial derivatives of the Helmholtz energy density:

$$\boldsymbol{M}\left(\boldsymbol{B},\boldsymbol{\varepsilon}\right) = -\left(\frac{\partial\psi\left(\boldsymbol{B},\boldsymbol{\varepsilon}\right)}{\partial\boldsymbol{B}}\right)^{\mathrm{T}} \tag{2}$$

$$\boldsymbol{\sigma}_{\mathrm{me}}\left(\boldsymbol{B},\boldsymbol{\varepsilon}\right) = \frac{\partial\psi\left(\boldsymbol{B},\boldsymbol{\varepsilon}\right)}{\partial\boldsymbol{\varepsilon}}. \tag{3}$$

The magnetic field strength is $\boldsymbol{H} = \nu_0\boldsymbol{B} - \boldsymbol{M}$, and the total stress $\boldsymbol{\sigma} = \boldsymbol{\sigma}_{\mathrm{me}} + \boldsymbol{\sigma}_{\mathrm{mag}}$ also includes the purely electromagnetic contribution from the Maxwell stress tensor

$$\boldsymbol{\sigma}_{\mathrm{mag}} = \nu_0\left(\boldsymbol{B}\boldsymbol{B}^{\mathrm{T}} - \frac{1}{2}\left(\boldsymbol{B}\cdot\boldsymbol{B}\right)\boldsymbol{I}\right) + \left(\boldsymbol{M}\cdot\boldsymbol{B}\right)\boldsymbol{I} - \boldsymbol{B}\boldsymbol{M}^{\mathrm{T}}, \tag{4}$$

in which $\nu_0 = 1/\mu_0$ is the reluctivity of free space.

The hysteretic behavior is modeled following the 2-D vector J-A hysteresis model comprehensively described in [7]. The magnetomechanical coupling is introduced in the model by iterating the anhysteretic magnetization $\boldsymbol{M}_{\mathrm{an}}$ for a given effective field strength $\boldsymbol{H}_{\mathrm{eff}}$ from the SV model (2) as

$$\boldsymbol{M}_{\mathrm{an}} = \boldsymbol{M}\left(\mu_0\left(\boldsymbol{H}_{\mathrm{eff}} + \boldsymbol{M}_{\mathrm{an}}\right),\boldsymbol{\varepsilon}\right). \tag{5}$$

The effect of stress on the coercive field strength is modeled by introducing stress-induced anisotropy to the J-A model pinning parameter k [7]. Instead of a scalar k, we use a diagonal tensor in the principal stress coordinates assuming that the diagonal terms depend only on the corresponding principal stresses σ_1 and σ_2. A second-order Taylor expansion around zero stress gives

$$\boldsymbol{k}_{12}\left(\boldsymbol{\sigma}_{12}\right) = k_0\left(\boldsymbol{I} + a\boldsymbol{\sigma}_{12} + b\boldsymbol{\sigma}_{12}^2\right) \text{ with } \boldsymbol{\sigma}_{12} = \begin{bmatrix}\sigma_1 & 0\\ 0 & \sigma_2\end{bmatrix}, \tag{6}$$

in which k_0, a and b are fitting parameters and $\boldsymbol{I}$ is the unit tensor. The derivative of the irreversible magnetization $\boldsymbol{M}_{\mathrm{irr}}$ with respect to the effective field strength is calculated by transforming the $\boldsymbol{k}_{12}$ tensor from the principal coordinates to the global xy-coordinate system as

$$\frac{d\boldsymbol{M}_{\mathrm{irr}}}{d\boldsymbol{H}_{\mathrm{eff}}} = \left(\boldsymbol{R}_\theta^{\mathrm{T}}\boldsymbol{k}_{12}\boldsymbol{R}_\theta\right)^{-1}\left(\boldsymbol{d}\boldsymbol{d}^{\mathrm{T}}\right) \text{ with } \boldsymbol{d} = \frac{\boldsymbol{M}_{\mathrm{an}} - \boldsymbol{M}_{\mathrm{irr}}}{\left|\boldsymbol{M}_{\mathrm{an}} - \boldsymbol{M}_{\mathrm{irr}}\right|} \tag{7}$$

in which the coordinate transformation matrix $\boldsymbol{R}_\theta$ and the first principal axis angle θ are

$$\boldsymbol{R}_\theta = \begin{bmatrix}\cos\theta & \sin\theta\\ -\sin\theta & \cos\theta\end{bmatrix} \text{ and } \theta = \frac{1}{2}\operatorname{atan}\frac{2\sigma_{\mathrm{xy}}}{\sigma_{\mathrm{xx}} - \sigma_{\mathrm{yy}}}. \tag{8}$$

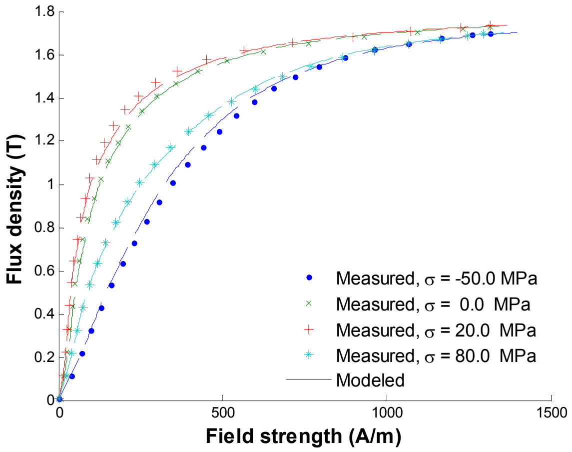

Fig. 1. Fitting the parameters of the single-valued model to *H*-averaged *B*-*H* curve measurements at different stresses.

III. Results and Discussion

Initial fitting results to unidirectional magnetization curve measurements under parallel uniaxial stresses are presented here. The magnetization curves have been measured for 0.5-mm nonoriented Fe-Si sheets under nine different stresses $\boldsymbol{\sigma}_{\mathrm{L}}$ ranging from 50 MPa compression (–) to 80 MPa tension (+). Fig. 1 shows results for fitting the SV model parameters [2] to the *H*-averaged magnetization loops at four different stress values. For a given load $\boldsymbol{\sigma}_{\mathrm{L}}$ and flux density $\boldsymbol{B}$, the total strain $\boldsymbol{\varepsilon}$ has been iterated from

$$\boldsymbol{\sigma}\left(\boldsymbol{B},\boldsymbol{\varepsilon}\right)-\boldsymbol{\sigma}_{\mathrm{L}}=\boldsymbol{0}\,. \tag{9}$$

It is emphasized that despite the unidirectional flux density and stress, using the vector model is essential since the perpendicular components of $\boldsymbol{\varepsilon}$ also become nonzero. The model fits reasonably well and is able to predict the quadratic dependency of the magnetization curves on the stress, so that both compression and high tension reduce the permeability from the zero-stress case. This effect is not observed with the energy definitions of [3] and [6].

Fig. 2 shows the results of fitting the J-A model parameters c and α [7], as well as the pinning tensor (6) to measured hysteresis loops and losses at the same four stresses. Both the loop shapes and the coercive fields are reasonably modeled. Finally, a good correspondence is observed in Fig. 3 between the measured and modeled hysteresis losses also at the other five stress values used in the measurements.

The initial results from the proposed model seem promising for predicting magnetization curves and hysteresis losses in mechanically loaded laminations. Choosing the flux density and total strain as the variables allows straightforward implementation of the model in FE formulations for the magnetic vector potential and mechanical displacement. In the full paper, we plan to study the properties of the model with both biaxial stresses and rotational flux densities. The chosen expression for the Helmholtz free energy will also be discussed in more details.

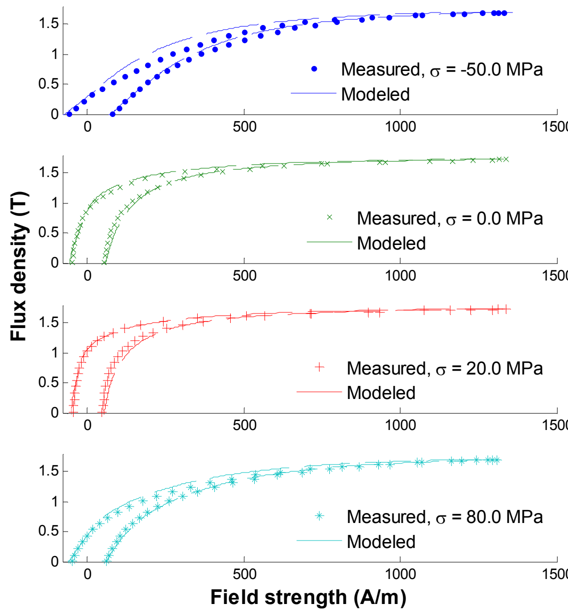

Fig. 2. Fitting the hysteresis model parameters to the *B*-*H* curve measurements at different stresses

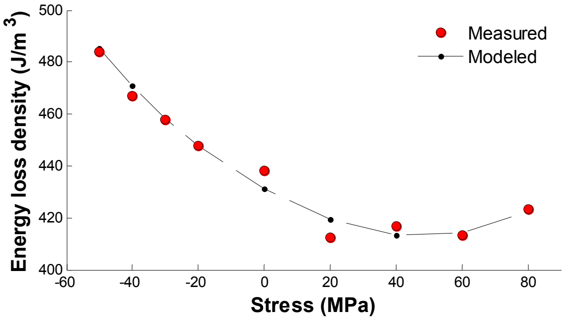

Fig. 3. Comparison of modeled and measured static hysteresis losses at different stresses.

References

[1] K. Fujisaki, R. Hirayama, T. Kawachi, S. Satou, C. Kaidou, M. Yabumoto, T. Kubota, “Motor Core Iron Loss Analysis Evaluating Shrink Fitting and Stamping by Finite-Element Method,” *IEEE Trans. Magn.*, Vol. 43, No. 5, pp. 1950-1954, 2007.

[2] K. Fonteyn, “Energy-Based Magneto-Mechanical Model for Electrical Steel Sheets,” Ph.D. thesis, Aalto University, Espoo, Finland, 2010. Available at: http://lib.tkk.fi/Diss/2010/isbn9789526032887.

[3] L. Bernard, X. Mininger, L. Daniel, G. Krebs, F. Bouillaut, M. Gabsi, “Effect of Stress on Switched Reluctance Motors: A Magneto-Elastic Finite-Element Approach Based on Multiscale Constitutive Laws,” *IEEE Trans. Magn.*, Vol. 47, No. 9, pp. 2171-2178, 2011.

[4] H. Ebrahimi, Y. Gao, H. Dozono, K. Muramatsu, “Coupled Magneto-Mechanical Analysis in Isotropic Materials Under Multiaxial Stress,” *IEEE Trans. Magn.*, Vol. 50, No. 2, 2014.

[5] D. Miyagi, N. Maeda, Y. Ozeki, K. Miki, N. Takahashi, “Estimation of Iron Loss in Motor Core With Shrink Fitting Using FEM Analysis,” *IEEE Trans. Magn.,* Vol. 45, No. 3, pp. 1704-1707, March 2009.

[6] L Bernard, X. Mininger, L. Daniel, J. V. Leite, N. Sadowski, N. J. Batistela, “A Jiles-Atherton based hysteresis model for magnetic materials under complex magneto-mechanical loadings,” COMPUMAG, Budapest, Hungary, June-July 2013.

[7] J. Gyselinck, P. Dular, N. Sadowski, J. Leite, J. P. A. Bastos, “Incorporation of a Jiles-Atherton vector hysteresis model in 2D FE magnetic field computations,” *COMPEL*, Vol. 23, No. 3, pp. 685-693, 2004.